HYDROLOGICAL PROCESSES
Hydrol. Process. **28**, 2630–2638 (2013)
Published online 19 April 2013 in Wiley Online Library
(wileyonlinelibrary.com) DOI: 10.1002/hyp.9837

Influence of river channel geometry in stream flow modelling and guidelines for field investigation

Hongbo Zhang,[1,2] Fan Zhang,[1,2]* Xiaonan Shi,[1,2] Chen Zeng,[1,2] Dong-Sin Shih,[3†] Gour-Tsyh Yeh[4] and Daniel R. Joswiak[1]

[1] *Key Laboratory of Tibetan Environment Changes and Land Surface Processes, Institute of Tibetan Plateau Research, Chinese Academy of Sciences, Beijing, China*
[2] *Key Laboratory of Alpine Ecology and Biodiversity, Institutes of Tibetan Plateau Research, Chinese Academy of Sciences, Beijing, China*
[3] *Taiwan Typhoon and Flood Research Institute, National Applied Research Laboratories, Taiwan*
[4] *Graduate Institute of Applied Geology, National Central University, Taiwan*

Abstract:

Fully physics-based, process-level, distributed fluid flow and reactive transport hydrological models are rarely used in practice until recent years. These models are useful tools to help understand the fundamental physical, chemical, and biological processes that take place in nature. In this study, sensitivity analyses based on a mountain area river basin modelling study are performed to investigate the effect of river channel geometric characteristics on downstream water flow. Numerical experiments show that reduction in the river channel geometric measurement interval may not significantly affect the downstream water stage simulation as long as measurement accuracy at special nodes is guaranteed. The special upstream nodes include but are not limited to 1) nodes located close to the observation station, 2) nodes near the borders of different land covers with considerable riverbed roughness changes, 3) nodes at entering points of tributaries causing discharge jump and 4) nodes with a narrow cross-section width that may control the flow conditions. This information provides guidelines for field investigation to efficiently obtain necessary geometric data for physics-based hydrological modelling. It is especially useful in alpine areas such as the Tibetan Plateau where field investigation capability is limited under severe topography and climate condition. Copyright © 2013 John Wiley & Sons, Ltd.

KEY WORDS distributed hydrological model; sensitivity analyses; river channel geometry; Tibetan Plateau

Received 17 September 2012; Accepted 18 March 2013

INTRODUCTION

Mountain area hydrological studies

Under global climate change scenarios, water bodies are undergoing dramatic changes in terms of temporal and spatial dimensions and multi-phase states (i.e. ice-water-vapor) transformations, which are especially significant in high-elevation mountain areas such as the Tibetan Plateau and surrounding mountains, referred to as the Third Pole. The unique atmosphere-cryosphere- hydrosphere interactions in the Third Pole region ensure permanent flows of Asia's major rivers, thus significantly influencing a fifth of the world's population in China, India, Nepal, Tajikistan, Pakistan, Afghanistan, Bhutan and so on. Recent climate change has a significant influence on the regional hydrological cycle in the Third Pole (Chen *et al*., 2007; Yao *et al*., 2007; Yao *et al*., 2012). Observational and modelling studies have reported a general trend of glacial retreat with increasing temperature (Yao *et al*., 2007; Li *et al*., 2008), increasing surface runoff from melting glaciers (Ye *et al*., 2003; Cyranoski, 2005), and rising lake water levers (Yao *et al*., 2004; Chen *et al*., 2007). Potential water resource problems in the region urgently require an improved understanding of the hydrological processes and the responses of the hydrological cycle to climate change.

Hydrological models are important tools for describing and predicting hydrological processes. They can be classified into four categories according to their structures and principles, that is, empirical models (e.g. Langbein *et al*., 1949; Stockton and Boggess, 1979; Revelle and Waggoner, 1983), water balance models (e.g. Thornthwaite and Mather, 1955; Gleick, 1987; Schaake and Waggoner, 1990), conceptual lumped models (e.g. Anderson, 1973; Burnash *et al*., 1973; Němec and Schaake, 1982; Ng and Marsalek, 1992), and process-based distributed models (e.g. Beven and Kirkby, 1979; Abbott *et al*., 1986;

*Correspondence to: Fan Zhang, Institute of Tibetan Plateau Research, Chinese Academy of Sciences, Beijing, China.
E-mail: zhangfan@itpcas.ac.cn
†Present Address: Department of Civil Engineering, National Chung Hsing University, Taiwan

Refsgaard and Storm, 1995; Schulla, 1997; Arnold *et al.*, 1998; Kollet and Maxwell, 2006; Camporese *et al.*, 2010; Yeh *et al.*, 2011). Among the four categories, the physically based distributed models give a more detailed and potentially more accurate description of the hydrological processes in a catchment compared with the other model types (Abbott and Refsgaard, 1996).

The needs and the concept for a physically based distributed catchment model were initially outlined by Freeze and Harlan (1969). Since the 1970s, a large number of other distributed models have been developed, such as TOPMODEL (Beven and Kirkby, 1979), MIKE SHE (Refsgaard and Storm, 1995), WaSiM-ETH (Schulla, 1997), SWAT (Arnold *et al.*, 1998), and WASH123D (Yeh *et al.*, 2011). According to the specific principles of each model, they are applied under different conditions.

Hydrological modelling of mountain area river basins

Recent hydrological models applied to the mountainous regions are typically the conceptual lumped models and the physics-based distributed models. For example, Yilmaz *et al.* (2011) implemented the conceptual lumped model ANN to predict catchment flow in a snow dominated mountainous basin named Karasu Basin, and the physics-based distributed model TOPOG was applied to an arid mountainous region in northwest China by Yu *et al.* (2010). Compared with empirical lumped models, which usually ignore the heterogeneity of the study area, the distributed models use parameters with physical meaning and have more capacity to handle hydrological processes in watersheds with significant topography and land cover changes.

However, it is difficult to obtain long-term hydrological data under the severe conditions of high-altitude mountain areas (Xue, 2005). Determination of water levels using automatic level gauges is more convenient and easier than on-site flow velocity measurements. Hydrological models which consider geometric dimension of river channels can simulate water level as well as flow rate (Orlandini and Rosso, 1998; Orlandini, 2002; Paz and Collischonn, 2007; Camporese *et al.*, 2010; Getirana, 2010). As a result, these models are capable of making use of water level data for flow simulation calibration and therefore save the cost and labor of multiple field trips to measure a wide range of flow velocity values. Alternatively, it is necessary to determine the geometric characteristics of river channels, including the river bed elevations and cross-sectional profiles (e.g. the river channel widths and depths) at certain intervals along the length of the river (Turcotte *et al.*, 2001; Ames *et al.*, 2009; Getirana, 2010).

Geometric information of rivers can be obtained by means of spot investigation and remote sensing methods (Winterbottom and Gilvear, 1997; Walsh *et al.*, 1998; Marcus *et al.*, 2003; Lejot *et al.*, 2007). Remote sensing techniques have been developed for telemetering major rivers, for example, the latest generation of high-resolution earth observation commercial satellites such as Ikonos, QuickBird, GeoEye-1, Landsat7, SPOT4, and CBERS-02B provide spatial resolutions ranging from 0.41 to 19.5 m. Therefore, remote sensing images still cannot give sufficiently accurate geometric information of small rivers (Jensen and Cowen, 1999; Zhang *et al.*, 2006; Wulder *et al.*, 2008). Consequently, efficiently obtaining necessary geometric information with limited field investigation capability becomes a key issue worthy of exploration for high-elevation river basin studies using physics-based, process-level distributed hydrological models. The objective of this study is to investigate the effect of upstream geometric characteristics on river/stream flow simulation and provide guidelines for relevant field investigations.

WASH123D MODEL

WASH123D is a multimedia, multi-processes, physics-based computational model (Yeh *et al.*, 2005; Yeh *et al.*, 2006). It can handle hydrological problems at the watershed scale with integrated media (river/stream networks, overland regime, and subsurface media) and processes (infiltration, evapotranspiration, recharge, moisture redistribution in vadose zone, groundwater flow, surface runoff, and river flow, etc.) (Figure 1). The model was designed to have the capability of simulating various

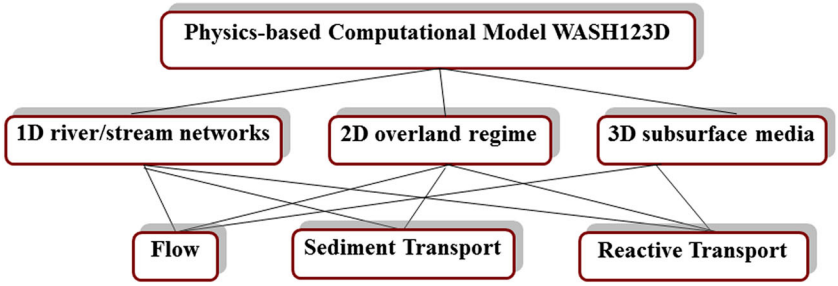

Figure 1. Description of WASH123D modelling capabilities

watershed system components or combinations of the components. It can simulate problems of various spatial and temporal scales as long as the assumptions of continuum are valid. Other versions of WASH123D were also developed for high-performance computing to enable the model to be efficient for large scale problems (Cheng *et al*., 2004a, b; Cheng *et al*., 2004a, b; Cheng *et al*., 2006).

The governing equations for water flow include both the Continuity Equation (1) based on the law of mass conservation and the Momentum Equation (2) based on the law of linear momentum conservation (Yeh *et al*., 2011):

$$\frac{\partial A}{\partial t}+\frac{\partial Q}{\partial S}=S_S+S_R-S_E+S_I+S_1+S_2 \qquad (1)$$

$$\frac{\partial Q}{\partial t}+\frac{\partial VQ}{\partial S}=-gA\frac{\partial(Z_0+h)}{\partial x}+(M_S+M_R-M_E+M_I+M_1+M_2)+\frac{B\tau^S-P\tau^b}{\rho} \qquad (2)$$

In the above equations, A is cross-sectional area; t is time; Q is flow rate; S is axis distance along the river; S_S, S_R, S_E, S_I, and S_1/S_2 are source/sinks because of artificial-introducing, rainfall, evapotranspiration, exfiltration and contributions from overland flow, respectively; V is flow velocity; g is gravity; Z_0 is riverbed elevation; h is water depth; M_S, M_R, M_E, M_I, M_1 and M_2 are momentum–impulses from the sources/sinks; B is top width of the cross-section; τ^S is surface shear stress; P is wet perimeter; τ^b is bottom shear stress affected by the Manning's roughness n; and ρ is water density. Three options including fully dynamic wave, diffusive wave and kinematic wave approaches are provided in WASH123D to solve the governing equations of water flow (Yeh *et al*., 2011).

BASE CASE: LANYANG CREEK BASIN HYDROLOGICAL MODELLING

The hydrological modelling in the Lanyang creek basin using WASH123D (Yeh *et al*., 2011) is proposed as a base case example. The river basin is located on the route followed by most typhoons making landfall during the summer typhoon season in Taiwan. It covers an area of approximately 978 km^2 and has a short hydrological response time due to its steep topography, which varies from 3740 m a.s.l. on the hilltops to sea level at the estuary.

The river basin of the Lanyang watershed is composed of three major streams, the Lanyang, Lotong and Dongshan, with the Lanyang stream being the main river draining this watershed. Among the two upstream reaches, the larger one discretized with 59 nodes was selected to perform numerical experiments. Calibrated simulation for Typhoon Nanmadol (3–4 December 2004) is used as base case for sensitivity analyses to investigate the applicability of WASH123D to high altitude river basins on the Tibetan Plateau, where limited geometric measurements can be provided for model parameterization. Simulation of the base case is compared with observations at the downstream hydrological station in Figure 2.

NUMERICAL EXPERIMENTS AND RESULTS

In WASH123D, the geometry of a river is described by three curves at each individual node, including the cross-section area, wetted perimeter and top width at different water depths. To investigate the influence of cross-section characteristics on downstream simulation results, a series of numerical experiments were designed through modifying the cross-section parameters of certain upstream nodes to check the sensitivity of downstream water stages simulated by WASH123D. The experiments can be divided into four sets. The first set is used to test the effect of measurement accuracy, and the other three sets are used to test the effect of both measurement accuracy and distance interval.

Experiment 1: single node cross-section width modification

A set of 58 numerical simulations were performed to investigate the effect of changing cross-section width at a single upstream node on the simulation of downstream flow. For each simulation, only geometric curves at one upstream node were modified to increase the cross-section width by 10%. The modified nodes range from node 1 to node 58. The simulation results of water stage curve at the downstream observation point (node 59) were compared with the base case by computing the coefficient of determination, that is, R^2 of river stages between the new simulation and the base case simulation. The R^2 values plotted in Figure 3 indicate the degree of difference between the new outputs and the base case.

Among all the upstream nodes, R^2 values corresponding to the change at eight ones (i.e. nodes 13, 14, 15, 16,

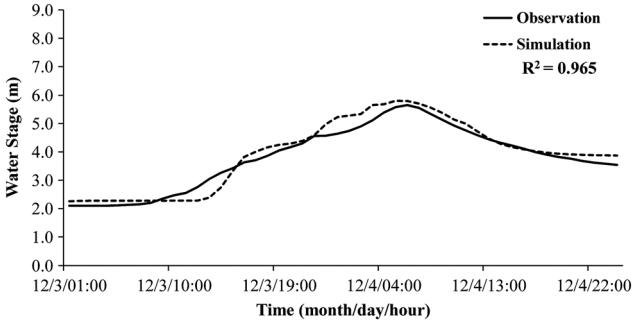

Figure 2. Base case simulated and observed water stages during Typhoon Nanmadol

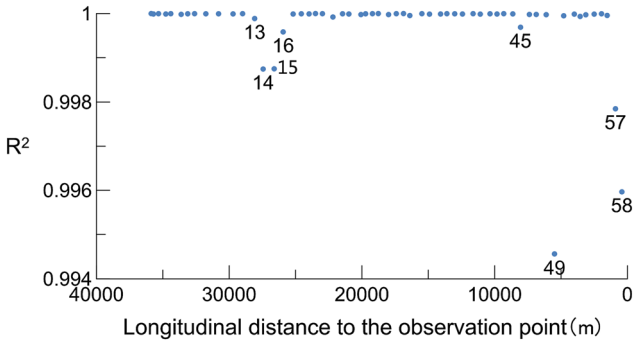

Figure 3. R^2 of experiment 1

45, 49, 57 and 58) are significantly smaller than the others. Among these special nodes, 57 and 58 are very close to the observation point (node 59) and thus affect the downstream flow more than the others.

To investigate the significance of the other six nodes, the distributions of riverbed elevation, land cover type (represented by specified Manning's n in the model) and peak discharge was examined. Figure 4 plots the riverbed elevation and land cover type distribution along the studied river reach. It is shown that the riverbed slope stays relatively constant along the reach and some of the special nodes, that is, nodes 13, 14, 15 and 16, are at the location where land cover changes from TYPE 1 to TYPE 2.

Figure 5 plots the simulated peak discharge distribution along the studied river reach. It is seen that there is a

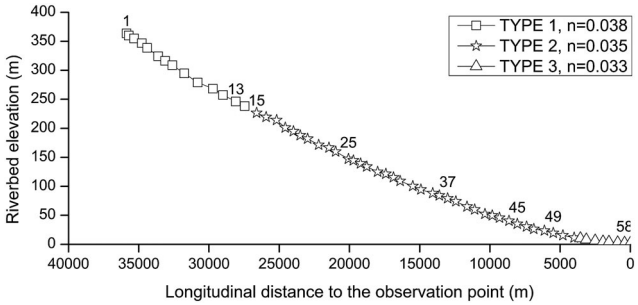

Figure 4. River bed elevation and land cover type distribution along the studied river reach

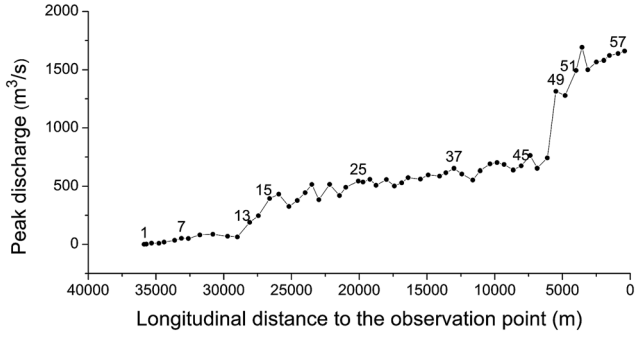

Figure 5. Simulated peak discharge distribution along the studied river reach

significant discharge jump at node 49 which is a junction of a small sub-branch.

To further investigate the reason why modification at node 45 can cause more changes of downstream flow than other nodes, Figure 6 plots the river channel width and water stage of peak discharge at node 45 and its neighboring nodes 44 and 46. It is seen that the river channel at node 45 is much narrower than both the upstream and the downstream neighboring nodes and thus may cause considerable water level increase and control the condition of the passing flow.

Because of the continuity of water depth along the river, abrupt changes in upstream water depths may affect the downstream water depths. According to the governing Equations (1) and (2) for water flow given in section 2, obvious variations in upstream parameters such as riverbed geometry (A, Z_0, B and P), flow rate (Q), source/sink terms (S_S, S_R, S_E, S_I, S_1, S_2, M_S, M_R, M_E, M_I, M_1 and M_2) and riverbed roughness (n) that may change the upstream water stage will influence the water stage observed at the downstream station.

Because the base case setting does not involve any source/sinks, the effect of riverbed geometry change at locations with source/sinks cannot be tested in this study. With that exception, results of Experiment 1 confirm that riverbed geometry changes at some special nodes influence the downstream water stage simulation more than at the other nodes. Similarly, these nodes include the following: (1) node 45 with an apparently narrower cross-section than its neighboring nodes, (2) node 49 at the junction of a sub-reach that causes a flow rate jump, (3) nodes 13, 14, 15 and 16 near the borders of different land covers with considerable riverbed roughness changes, and (4) nodes 57 and 58 located close to the observation station.

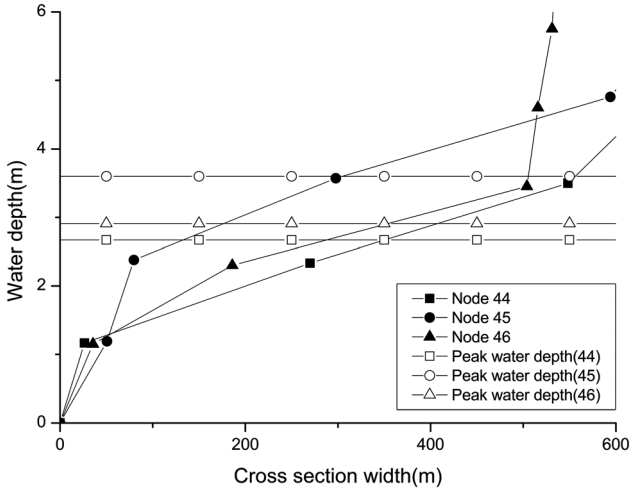

Figure 6. River channel width and water stage of peak discharge at nodes 44, 45 and 46

Experiment 2: cross-section measurement interval increased by two times

A set of 29 numerical simulations were performed to investigate the effect of changing cross-section characteristics of a single upstream node on the simulation of downstream flow rate. For each simulation, cross-section parameters of one odd-numbered node (including nodes 1, 3, 5, …, 57) were modified to be the same as its neighboring downstream node (i.e. nodes 2, 4, 6, …, 58, respectively). In this case, only half of the geometric information can be provided with doubled measurement interval. To compare the new simulation with the base case, R^2 values are plotted in Figure 7.

It can be observed that cross-section parameter modification of five nodes (nodes 13, 45, 49, 51 and 57) changed the simulation results dramatically more than modification of other nodes. All of these five nodes were among the special nodes identified by experiment set 1.

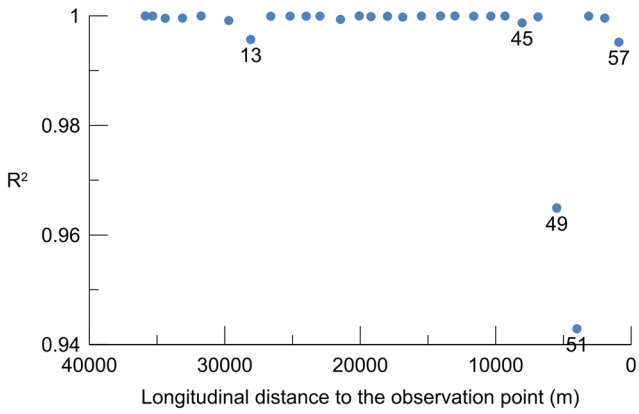

Figure 7. R^2 of experiment 2

The tests were then performed in another way. As shown in Figure 8, all the nodes are divided into five groups: nodes 1–12, nodes 13–24, nodes 25–36, nodes 37–48 and nodes 49–58. Similarly, cross-section parameters of nodes with odd numbers (such as node 1, 3, 5, …, 57) were modified to be the same as their neighboring downstream nodes (such as node 2, 4, 6, …, 58, respectively). However, modifications were made in groups, that is, measurement interval of the cross-section characteristics of one group of nodes were doubled as described above for each simulation.

R^2 values for the five simulations compared with the base case are listed in Table I

For comparison, another set of 5 simulations, that is, cases A2' through E2' (Figure 8 and Table II), were performed in the same way as cases A2 through E2, respectively, but without changing any of the special nodes (i.e. nodes 13, 45, 49, 51 and 57).

It can be observed that when geometric parameters of special nodes were unaltered, increasing the river channel measurement interval by 2 caused very little changes in the downstream flow simulation. Therefore, selectively increasing the river channel measurement interval can still maintain the accuracy of downstream simulation results.

Experiment 3: increasing cross-section measurement interval by three times

A set of 19 numerical simulations were performed to investigate the effect of changing cross-section characteristics of two neighboring upstream nodes simultaneously on the simulation of downstream flow rate. For each

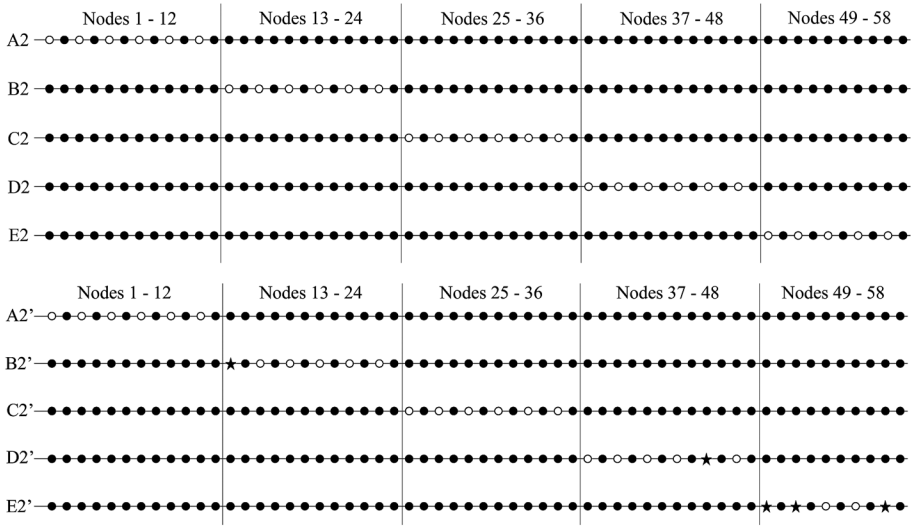

Figure 8. Modification to the base case in cases A2–E2 and A2'–E2'. Circles represent nodes at which cross-section parameters were modified to be the same as the neighboring downstream nodes. Black dots represent nodes at which cross-section parameters need to be measured for the simulation. Stars represent the special nodes at which cross-section parameters also need to be measured for the simulation.

Table I. Description of cases A2–E2

Case	Modified node range	Modified nodes	R^2
A2	1–12	Nodes 1, 3, ... through 52	0.99989
B2	13–24	Nodes 13, 15,... through 64	0.98754
C2	25–36	Nodes 25, 27 ... through 76	0.99991
D2	37–48	Nodes 37, 39, ... through 88	0.99731
E2	49–58	Nodes 49, 51, ... through 57	0.83548

Table II. Description of cases A2'-E2'

Case	Modified node range	Skipped nodes	R^2
A2'	1–12	None	0.99989
B2'	13–24	Node 13	0.99812
C2'	25–36	None	0.99991
D2'	37–48	Node 45	0.99990
E2'	49–58	Nodes 49, 51 and 57	0.99923

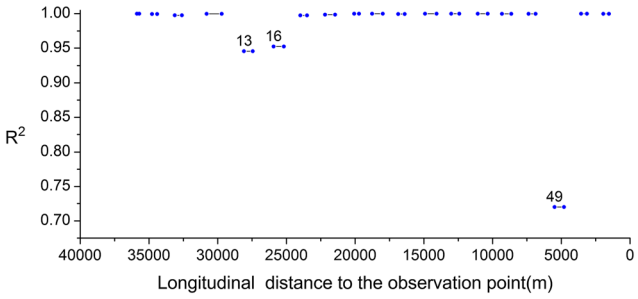

Figure 9. R^2 of experiment 3

simulation, cross-section parameters of two neighboring nodes (including nodes 1 and 2, 4 and 5; ...; 55 and 56) were modified to be the same as their neighboring downstream nodes (i.e. nodes 3, 6, ..., 57, respectively). In this case, only one-third of the geometric information can be provided with a tripled measurement interval. To compare the new simulation with the base case, R^2 values are plotted in Figure 9.

It can be observed that cross-section parameter modification of three sets of nodes (nodes 13 and 14, nodes 16 and 17, and nodes 49 and 50) changed the simulation results much more than modification of other sets of nodes. Each of these three sets contains at least one special node identified in experiment set E1, that is, nodes 13, 14, 16 and 49.

Similar to section 4.2, modifications were then performed in five groups (cases A3–E3) as described in Figure 10 and Table III. Alternatively, the modification tripled the measurement interval of cross-section characteristics group by group. R^2 values for each simulation compared with the base case are also listed in Table III.

For comparison, another set of simulations, that is, cases A3' through E3' (Figure 10 and Table IV), was performed in the same way as cases A3 through E3, respectively, but without changing the special nodes.

Similar to section 4.2, when skipping the special nodes, little changes in the downstream flow simulation were observed with the increase of river channel measurement interval.

Experiment E4: extreme cases

Finally, a set of extreme experiments were conducted to test the extent of influence of cross-section parameters.

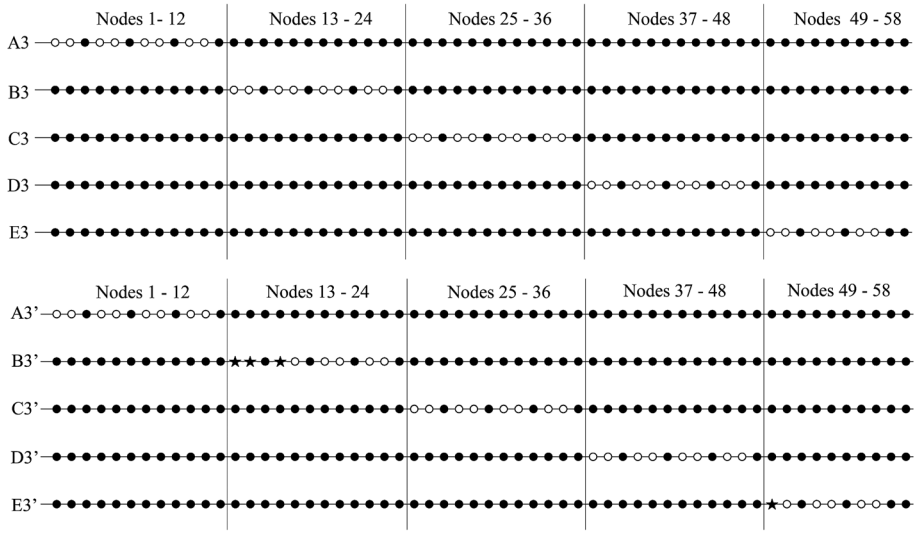

Figure 10. Modification to the base case in cases A3–E3 and A3'–E3'. Circles represent nodes at which cross-section parameters were modified to be the same as the neighboring downstream nodes. Black dots represent nodes at which cross-section parameters need to be measured for the simulation. Stars represent the special nodes at which cross-section parameters also need to be measured for the simulation

Table III. Description of cases A3–E3

Case	Modified node range	Modified nodes	R^2
A3	1–12	Nodes 1 and 2, 4 and 5, ... through 10 and 11	0.99976
B3	13–24	Nodes 13 and 14, 16 and 17, ... through 22 and 23	0.95482
C3	25–36	Nodes 25 and 26, 28 and 29, ... through 34 and 35	0.99974
D3	37–48	Nodes 37 and 38, 40 and 41, ... through 46 and 47	0.99945
E3	49–58	Nodes 49 and 50, 52 and 53, and 55 and 56	0.70449

Table IV. Description of study cases A3'–E3'

Case	Modified node range	Skipped nodes	R^2
A3'	1–12	None	0.99976
B3'	13–24	Nodes 13,14,16	0.99957
C3'	25–36	None	0.99922
D3'	37–48	None	0.99742
E3'	49–58	Node 49	0.99802

Table V. Description of cases A4–D4

Case	Range	Skipped nodes	R^2
A4	1–12	None	0.99475
B4	1–44	Nodes 13,14,15,16	0.96961
C4	1–48	Nodes 13,14,15,16,45	0.97487
D4	1–58	Nodes 13,14,15,16,45,49, 57, 58	0.96923

According to the previous experiments, four types of special nodes were identified, including (1) nodes 57 and 58 located close to the observation station (within ~100m), (2) nodes 13, 14, 15, 16 near the borders of different land covers with considerable riverbed roughness changes (8.57%), (3) node 49 at a junction of subreaches causing a discharge jump (77% in this study), and (4) node 45 with narrow cross-section (<87% of neighboring nodes) that may control the flow condition. The extreme tests are performed by modifying cross-section characteristic curves of upstream nodes but skipping the modification of these four types of special nodes.

As shown in Figure 11, we firstly performed simulation A4 by changing the cross-section characteristics of nodes 1–12 to be the same as node 13. Second, simulation B4 was performed on the basis of A4 with additional changes of nodes 17–44 to have the same cross-section curves as node 45. Third, simulation C4 was performed based on B4 with additional changes of nodes 46–48 to have the same cross-section curves as node 49. Finally, simulation D4 was performed based on C4 with additional changes of nodes 50–56 to have the same cross-section curves as node 57. R^2 values for these simulations compared to the base case are listed in Table V.

It can be observed that, with modifications carrying forward from upstream to downstream, the R^2 values were reduced, whereas all the simulation results are relatively acceptable with the minimum > 0.96. In other words, as long as we can precisely identify the river channel geometry of the special nodes, decrease in the precision of the other nodes' cross-section measurements do not significantly change the simulation results.

DISCUSSION AND CONCLUSION

River flow calculated from local measurements, such as bed material particle size, hydraulic depth and riverbed slope, may not be accurate (Orlandini, 2002). Through

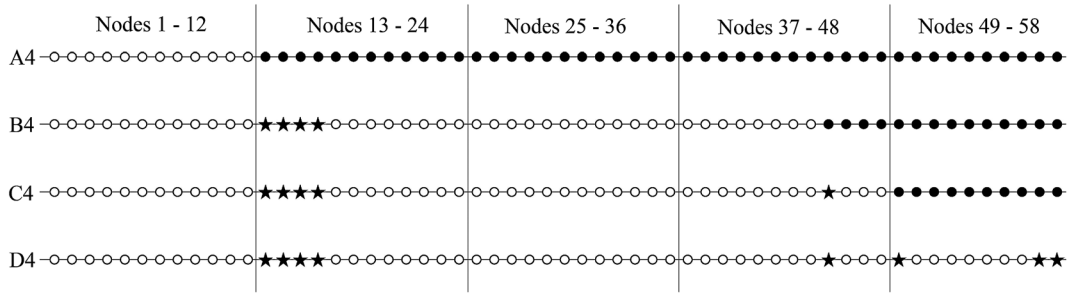

Figure 11. Modification to the base case in cases A4–D4. Circles represent nodes at which cross-section parameters were modified to be the same as the neighboring downstream nodes. Black dots represent nodes at which cross-section parameters need to be measured for the simulation. Stars represent the special nodes at which cross-section parameters also need to be measured for the simulation

numerical experiments using distributed hydrological model based on the laws of mass conservation and linear momentum conservation, this study investigated the effect of upstream river channel geometry on the downstream flow calculation. Results show that increasing the cross-section measurement interval does not significantly affect the performance of the downstream flow simulation as long as accuracy at special nodes is guaranteed. The special nodes may include but are not limited to the following: (1) nodes located close to the observation station, (2) nodes near the borders of different land covers with considerable riverbed roughness changes, (3) nodes at junctions of sub-reaches causing discharge jumps, and (4) nodes with narrow cross-section that may control flow conditions.

It should be noted that the above conclusions drawn from the numerical experiments depend on the complexity of the base case setting. For example, the effect of riverbed geometry at locations with source/sink or significant river-bed slope change cannot be tested in the case study because the base case setting does not involve source/sinks and the bed slope is generally consistent along the river.

This study provides some preliminary guidelines for data collection arrangement. To provide sufficient geometric data for precise river/stream water stage simulation using the physically based distributed hydrological model, river channel geometric information at the special nodes mentioned above must be measured accurately. Additional measurements at certain distance intervals along the river/stream should be arranged considering the field investigation capability.

ACKNOWLEDGEMENT

This research was supported by the National Natural Science Foundation of China (41001034 and 41190082).

REFERENCES

Abbott MB, Refsgaard JC. 1996. Distributed hydrological modelling, Springer.

Abbott MB, Bathurst JC, Cunge JA, O'Connell PE, Rasmussen J. 1986. An introduction to the European hydrological system--Systeme Hydrologique Europeen. *Journal of Hydrology* **87**(1–2): 45–59.

Ames DP, Rafn EB, Van Kirk R, Crosby B. 2009. Estimation of stream channel geometry in Idaho using GIS-derived watershed characteristics. *Environmental Modelling & Software* **24**(3): 444–448.

Anderson EA. 1973. National Weather Service river forecast system--snow accumulation and ablation model. TECHNICAL MEMORANDUM NWS HYDRO-17, NOVEMBER 1973. 217 P.

Arnold JG, Srinivasan R, Muttiah RS, Williams J. 1998. Large area hydrologic modeling and assessment part I: Model development1. *JAWRA Journal of the American Water Resources Association* **34**(1): 73–89.

Beven K, Kirkby M. 1979. A Physically Based, Variable Contributing Area Model of Basin Hydrology. *Hydrological Sciences Bulletin* **24**(1): 43–69.

Burnash RJC, Ferral RL, McGuire RA. 1973. A generalized streamflow simulation system: conceptual modeling for digital computers, US Dept. of Commerce, National Weather Service.

Camporese M, Paniconi C, Putti M, Orlandini S. 2010. Surface-subsurface flow modeling with path-based runoff routing, boundary condition-based coupling, and assimilation of multisource observation data. *Water Resources Research* **46**(2): W02512.

Chen X, Cui P, Li Y, Yang Z, Qi Y. 2007. Changes in glacial lakes and glaciers of post-1986 in the Poiqu River basin, Nyalam, Xizang (Tibet). *Geomorphology* **88**(3–4): 298–311.

Cheng HP, Lin H, Edris E, McVan D, Tate C, Sanchez J, Jackson A, McGehee T, Kokkanti P, Ketprakong N. 2004a. Biscayne Bay coastal wetlands and C-111 spreader canal conceptual model technical memorandum (task 1). *US Army Corps of Engineers Engineer Research and Development Center* **3909**: 39180–36199.

Cheng JRC, Lin HC, Cheng HW, Hunter RM, Richards DR, Yeh GT. 2004b. Parallelization of the WASH123D code – phase I: 2-dimensional overland and 3-dimensional subsurface flow. Proc. XV International conference on computational methods in water resources.: 1403–1413.

Cheng JR, Hunter RM, Cheng HP, Richards DR, Yeh GT. 2006. Parallelization of the WASH123D code—phase III: 1-dimensional channel, 2-dimensional overland, and 3-dimensional subsurface flows. XVI international conference on computational methods in water resources. B. P, E. P, D. H, G. WG,P. G.

Cyranoski D. 2005. Climate change: The long-range forecast. *Nature* **438**: 275–276.

Freeze RA, Harlan R. 1969. Blueprint for a physically-based, digitally-simulated hydrologic response model. *Journal of Hydrology* **9**(3): 237–258.

Getirana ACV. 2010. Integrating spatial altimetry data into the automatic calibration of hydrological models. *Journal of Hydrology* **387**(3): 244–255.

Gleick PH. 1987. The development and testing of a water balance model for climate impact assessment: modeling the Sacramento basin. *Water Resources Research* **23**(6): 1049–1061.

Jensen JR, Cowen DC. 1999. Remote sensing of urban/suburban infrastructure and socio-economic attributes. *Photogrammetric Engineering and Remote Sensing* **65**: 611–622.

Kollet SJ, Maxwell RM. 2006. Integrated surface-groundwater flow modeling: A free-surface overland flow boundary condition in a parallel groundwater flow model. *Advances Water Resources* **29**(7): 945–958.

Langbein WB, *et al*. 1949. Annual Runoff in the United States. Washington, D.C., U.S. Department of Interior.

Lejot J, Delacourt C, Piegay H, Fournier T, Trémélo ML, Allemand P. 2007. Very high spatial resolution imagery for channel bathymetry and topography from an unmanned mapping controlled platform. *Earth Surface Processes and Landforms* **32**(11): 1705–1725.

Li X, Cheng G, Jin H, Kang E, Che T, Jin R, Wu L, Nan Z, Wang J, Shen Y. 2008. Cryospheric change in China. *Global and Planetary Change* **62**(3): 210–218.

Marcus WA, Legleiter CJ, Aspinall RJ, Boardman JW, Crabtree RL. 2003. High spatial resolution hyperspectral mapping of in-stream habitats, depths, and woody debris in mountain streams. *Geomorphology* **55**(1): 363–380.

Němec J, Schaake J. 1982. Sensitivity of water resource systems to climate variation/Sensibilité des systèmes de ressources en eau aux variations climatiques. *Hydrological Sciences Journal* **27**(3): 327–343.

Ng H, Marsalek J. 1992. Sensitivity of streamflow simulation to changes in climatic inputs. *Nordic Hydrology* **23**(4): 257–272.

Orlandini S. 2002. On the spatial variation of resistance to flow in upland channel networks. *Water Resources Research* **38**(10): 1197.

Orlandini S, Rosso R. 1998. Parameterization of stream channel geometry in the distributed modeling of catchment dynamics. *Water Resources Research* **34**(8): 1971–1985.

Paz AR, Collischonn W. 2007. River reach length and slope estimates for large-scale hydrological models based on a relatively high-resolution digital elevation model. *Journal of Hydrology* **343**(3–4): 127–139.

Refsgaard JC, Storm B. 1995. *Computer Models of Watershed Hydrology*. Water Resources Publications: Englewood, USA.

Revelle RR, Waggoner PE. 1983. Effects of a Carbon Dioxide-Induced Climatic Change on Water Supplies in 7 the Western United States. *Month* **419**: 432.

Schaake JC, Waggoner P. 1990. From climate to flow." Climate change and US water resources.: 177–206.

Schulla. 1997. Hydrologische Modellierung von Fliessgebieten zur Abschätzung der Folgen von Klimaänderungen, Verlag Geographisches Institut ETH Zürich.

Stockton CW, Boggess WR. 1979. Geohydrological implications of climate change on water resource development. Fort Belvoir, VA, U.S. Army Coastal ResearchEngineering Center.

Thornthwaite CW, Mather JR. 1955. The Water Balance. Users Manual for HydrologicalSimulation Program-FORTRAN (HSPF).

Turcotte R, Fortin JP, Rousseau A, Massicotte S, Villeneuve JP. 2001. Determination of the drainage structure of a watershed using a digital elevation model and a digital river and lake network. *Journal of Hydrology* **240**(3): 225–242.

Walsh SJ, Butler DR, Malanson GP. 1998. An overview of scale, pattern, process relationships in geomorphology: a remote sensing and GIS perspective. *Geomorphology* **21**(3): 183–205.

Winterbottom SJ, Gilvear DJ. 1997. Quantification of channel bed morphology in gravel-bed rivers using airborne multispectral imagery and aerial photography. *Regulated Rivers: Research & Management* **13**(6): 489–499.

Wulder MA, White JC, Coops NC, Butson CR. 2008. Multi-temporal analysis of high spatial resolution imagery for disturbance monitoring. *Remote Sensing of Environment* **112**(6): 2729–2740.

Xue J-S. 2005. Some Scientific Issues on Numerical Weather Prediction in Northwest China [J]. *Journal of Arid Meteorology* **23**(1): 68–71.

Yao T, Wang Y, Liu S, Pu J, Shen Y, Lu A. 2004. Recent glacial retreat in High Asia in China and its impact on water resource in Northwest China. *Science in China Series D: Earth Sciences* **47**(12): 1065–1075.

Yao T, Pu J, Lu A, Wang Y, Yu W. 2007. Recent glacial retreat and its impact on hydrological processes on the Tibetan Plateau, China, and surrounding regions. *Arctic, Antarctic, and Alpine Research* **39**(4): 642–650.

Yao TD, Thompson LG, Mosbrugger V, Zhang F, Ma Y, Luo T, Xu B, Yang X, Joswiak DR, Wang W, Joswiak ME, Devkota LP, Tayal S, Jilani R, Fayziev R. 2012. Third Pole Environment (TPE). *Environmental Development* **3**: 52–64.

Ye B, Yongjian D, Fengjing L, Caohai L. 2003. Responses of various-sized alpine glaciers and runoff to climatic change. *Journal of Glaciology* **49**(164): 1–7.

Yeh GT, Huang GB, Cheng HP, Zhang F, Lin HC, Edris E, Richards D. 2006. A first principle, physics based watershed model: WASH123D. Watershed Models. Singh VP and Frevert. DK: 211–244.

Yeh GT, Shih DS, Cheng JRC. 2011. An integrated media, integrated processes watershed model. *Computers & Fluids* **45**(1): 2–13.

Yeh GT, Huang GB, Zhang F, Cheng HP, Lin HC. 2005. WASH123D: a numerical model of flow, thermal transport, and salinity, sediment, and water quality transport inWAterSHed systems of 1-D stream-river network, 2-D overland regime, and 3-D subsurface media, Department of Civil and Environmental Engineering, University of Central Florida.

Yilmaz AG, Imteaz MA, Jenkins G. 2011. Catchment flow estimation using Artificial Neural Networks in the mountainous Euphrates Basin. *Journal of Hydrology* **410**: 134–140.

Yu P, Wang Y, Wu X, Dong X, Xiong W, Bu G, Wang S, Wang J, Liu X, Xu L. 2010. Water yield reduction due to forestation in arid mountainous regions, northwest China. *International Journal of Sediment Research* **25**(4): 423–430.

Zhang T, Tang J, Liu D. 2006. Feasibility of Satellite Remote Sensing Image About Spatial Resolution [J]. *Journal of Earth Sciences and Environment* **1**: 79–82.

